Scientific Research Publishing

Open Journal of Modelling and Simulation, 2022, 10, 255-266
https://www.scirp.org/journal/ojmsi
ISSN Online: 2327-4026
ISSN Print: 2327-4018

Numerical Simulation of CFD and Fluid-Structure-Interaction (FSI) of Steady Flow in a Stenotic Vessel

Md. Jashim Uddin[1*], Md. Sayeed Iftekhar Yousuf[2]

[1]Department of Applied Mathematics, Noakhali Science and Technology University, Noakhali, Bangladesh
[2]Department of Computer Science and Mathematics, Bangladesh Agricultural University, Mymensingh, Bangladesh
Email: *mdjaud11@gmail.com

How to cite this paper: Uddin, M.J. and Yousuf, M.S.I. (2022) Numerical Simulation of CFD and Fluid-Structure-Interaction (FSI) of Steady Flow in a Stenotic Vessel. *Open Journal of Modelling and Simulation*, **10**, 255-266.
https://doi.org/10.4236/ojmsi.2022.103013

Received: April 21, 2022
Accepted: May 28, 2022
Published: May 31, 2022

Abstract

This paper is concerned with the computational results of two-dimensional axisymmetric rigid and elastic wall formulation. In this paper, steady flow in a stenotic vessel is simulated and compared to available numerical data with COMSOL Multiphysics software. Numerical results for a 2D axisymmetric vessel of 45% area reduction indicate that as the area is reduced with the decreasing of cross-section, the maximum axial velocity at post stenotic decreases until the end of the artery but the radial velocity increases upto 4 mm from the stenosis throat and then decreases. Overall, comparison is carried out on hemodynamics for elastic and rigid wall of steady flow. Our investigated findings may enable risk factor for patients with attacked cardiovascular diseases and can play an important role to detect a solution to such kinds of diseases.

Keywords

CFD, FSI, Steady Flow, Hemodynamic

1. Introduction

One of the major goals summarized in the United Nations 2030 work plan for sustainable development is to minimize one-third of the ill-timed departures from non-communicable diseases [1]. The globe's most general non-communicable diseases are cardio-vascular-diseases (CVDs), with over 50% of such kinds of deaths happening in low and intermediate-income countries in 2017, with the deaths of 17.8 million in 2017 [2]. Arterial blockage conducts to an important change in the parameters of blood flow. In most cases, blood flows are assumed

as laminar [3]. Due to maximum velocity of blood flow at the stenosis throat, there may grow high shear stress that leads to dangerous damage to the walls of artery. This affects the blood flow behaviors [4]. The disease happened by arterial blockage is known as atherosclerosis [5] which is one of the most worldwide diseases of the cardiovascular system all over the world. The leading reasons for death in the global are owing to the diseases of heart such as atherosclerosis [6]. Vessels of blood carry high cholesterols in the form of low-density lipoprotein [LDL] molecules for a long time [7]. Zingaro *et al.* [8] detected the endocardium motion and established the electromechanics-fluid dynamics model with one-way coupled in the left ventricle using Resistive Immersed Implicit Surface method. Ibrahim [9] explains that seminal fluid velocity is reduced with a growth in viscosity-dependent parameter. This contribution can be implemented in regulating spermatozoa transport into the cervical canal. Kim *et al.* [10] studied steady laminar and turbulent flow in a 2D model for the complete artificial heart.

The investigation and research analysis executed is a comparative one. The comparison has been conducted for the steady nature of assumed blood flow between the rigid and elastic walls to confirm a more accurate result. The computational results of blood flow speed, pressure drop and wall shear stress are all investigated. Our studied findings can enable risk factor for patients with attacked cardiovascular diseases and may play a crucial role to provide a solution to such kinds of diseases. The perfection and inferences would be laid down from the validity of computational results.

2. Computational Methodology

In this study, steady, isothermal, incompressible and Newtonian blood flows in two-dimensional axisymmetric vessel have been assumed. The artery walls have been considered to be smooth, rigid and flexible. This simulation is aimed to comprehend the flow in the stenotic vessel, and therefore, the radius of the artery is considered 2.5 mm (**Figure 1**) and total artery length is 65 mm. The density and viscosity of the fluid are 755 kg/m^3 and 0.00143 Pa·s, respectively. The effect of gravity is negligible. The mass and momentum conservation equations can be given as follows.

Continuity equation:

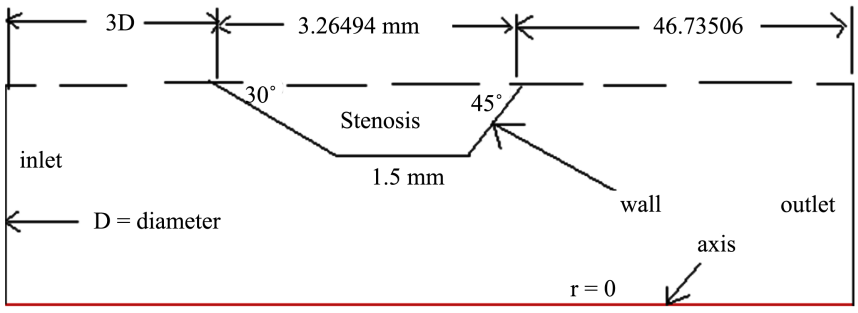

Figure 1. Computational diagram.

$$\nabla \cdot u = 0 \tag{1}$$

Momentum conservation equation:

$$\rho(u \cdot \nabla)u = -\nabla p + \nabla \cdot \left[\mu \left\{ \nabla u + (\nabla u)^{\mathrm{T}} \right\} \right] \tag{2}$$

where $\tau = \mu \left\{ \nabla u + (\nabla u)^{\mathrm{T}} \right\}$, u is identified by the velocity vector, pressure is p, ρ and μ are the density and dynamic viscosity respectively.

At the inlet section of the vessel, a constant velocity of 0.22 m/s ($\mathrm{Re} = 575$) having a parabolic profile corresponding to Poiseuille flow is imputed. At the outlet of the artery, constant pressure of 4140 Pa is fixed. No-slip boundary condition is marked on the artery wall. Another wall is considered to be isotropic and linearly flexible with Young's modulus ($E = 5 \times 10^5$ Pa), Poisson's ratio ($\upsilon = 0.499$) and wall density ($\rho_s = 10^3\ \mathrm{kg/m^3}$). The relative tolerance is set to 0.001. The direct solver is used for the solution. The solver method has chosen the Implicit Backward Differentiation Formula (BDF) for the computational results.

3. Results and Discussion

A computational grid consisting of triangular elements has been used for the simulation. A grid independence test has been conducted for constructing the accuracy of the solution. It is observed that the result becomes independent of the mesh size having 92,400 elements because maximum wall shear stress (WSS) remains constant between 92,400 and 193,883 elements (Figure 2). So the conclusive grid constitutes 92,400 elements.

The current numerical simulations model is validated with the computational investigations of Kang *et al.* [11] with taking identical properties. Here the comparison matches very well and as displayed in Figure 3(a) and Figure 3(b).

Figure 4 indicates the change in axial velocity in rigid and elastic walls at 45% area reduction. The axial velocity is almost similar (0.44 m/s) at upstream of the stenosis due to fully developed flow. However, the values drastically vary and distinctive axial velocities with rapid change in magnitudes are also noticed at

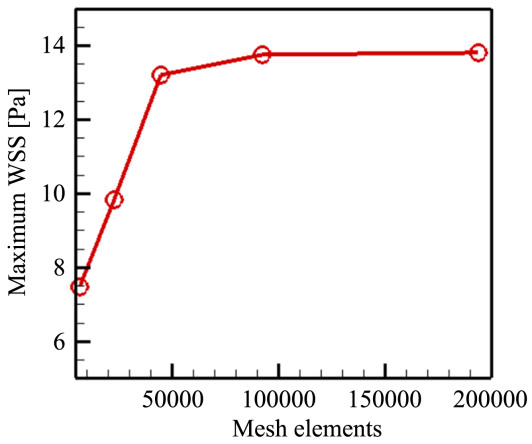

Figure 2. Grid test.

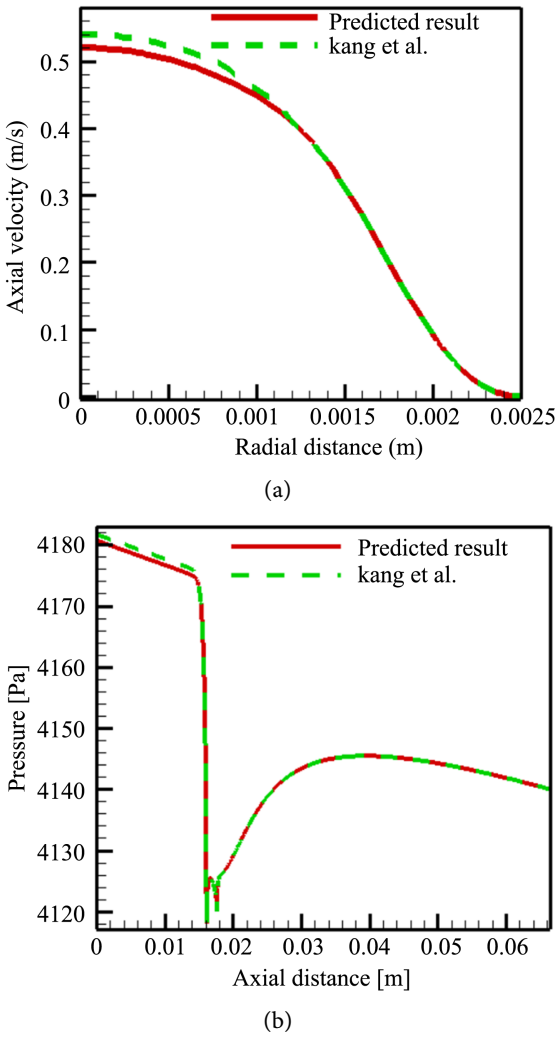

Figure 3. Numerical validation of (a) axial velocity distribution in the radial direction at x = 0.0216 m and (b) wall pressure distribution in the axial direction at the center for steady flow with Kang *et al.*

the stenotic of the lumen as well. It is mentionable that axial velocity varies between rigid and flexible walls of stenotic artery. The velocity finally generates a three-dimensional twisting impact on the steady blood flow. The severity of the twisting impact rises in downstream. Maximum axial velocity decreases as the axial distance increases from stenosis middle (**Figure 5**). The recirculation zone is noticeable upto 8 mm from the stenosis throat and it is negligible at 10 mm (**Figure 4** and **Figure 6**).

The effect on the radial velocity in the stenotic artery is displayed in **Figure 7**. The maximum radial velocity is almost stable and zero at the upstream site of the constriction (**Figure 7(a)** and **Figure 7(b)**). However, in the artery, there is a little peak in the radial velocity at the area of reduced lumen (**Figure 7(c)**). The radial velocity increases downstream of the stenosis at a distance of 4 mm from the stenosis middle (**Figure 7(d)** and **Figure 7(e)**) and then decreases until the end of the lumen (**Figure 7(f)** and **Figure 7(g)** and **Figure 7(h)**) and it is also

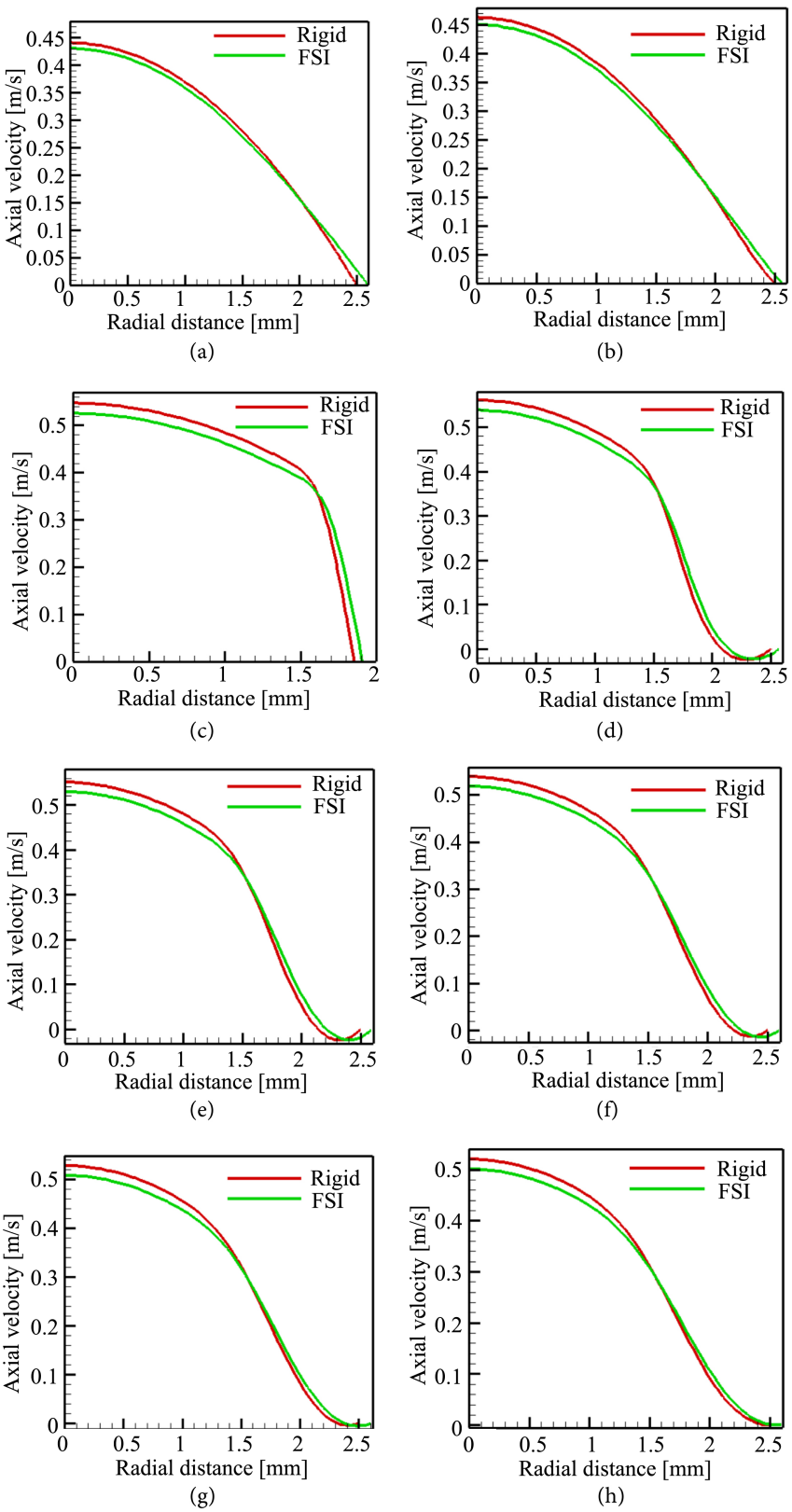

Figure 4. Axial velocity on upstream as a distance of 4 mm, 2 mm and 0 mm ((a), (b), (c)) and post stenotic zone as a distance of 2 mm, 4 mm, 6 mm, 8 mm and 10 mm ((d), (e), (f), (g), (h)) from stenosis throat of rigid and flexible walls.

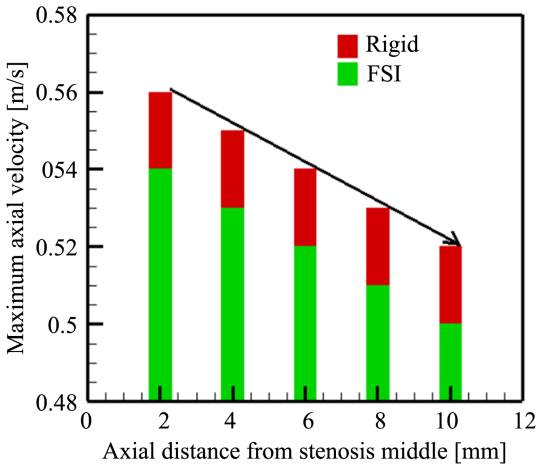

Figure 5. Maximum axial velocity at post stenotic area for rigid and elastic walls.

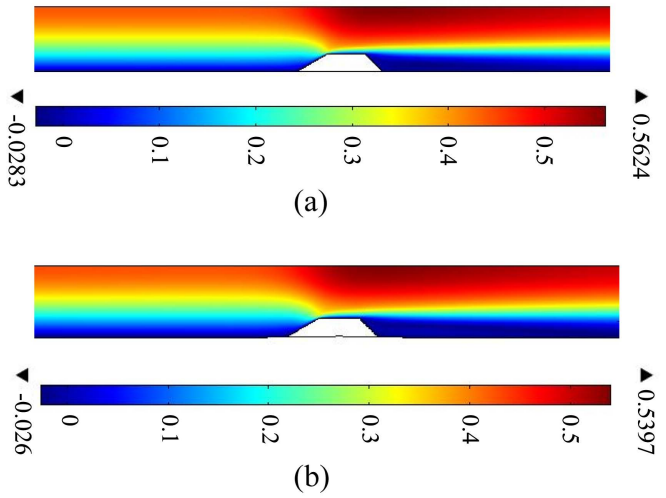

Figure 6. Axial velocity of rigid (a) and elastic walls (b) through the surface plot.

visible in **Figure 8**. The radial velocity in the vessel shows similar patterns compared to rigid and elastic walls of the artery but difference in magnitude. The maximum radial velocity of rigid and elastic wall arteries is 0.0113 m/s and 0.0108 m/s. It is significant to notify that the radial velocity is positively linked to the cross-sectional area reduction of the vessel (**Figure 7** and **Figure 9**). A positive connection of radial velocity with the narrowed lumen was found by Kanai *et al.* [12].

The effect on overall pressure in the stenotic modeled vessels is shown in **Figure 10** and **Figure 11** for both walls. The distribution of pressure in the considered blood vessel wall is rambling and segmental. Moreover, the pressure at the entry section is overall higher than the outlet. Pressure drop is observed at the stenosis location. A maximum pressure drop of 54 Pa is found in rigid wall while the less pressure drop of 44 Pa is found in the case of elastic wall of steady flow. The variation in pressure before and after the blockage is also lighted in the contour plot of pressure (**Figure 11**).

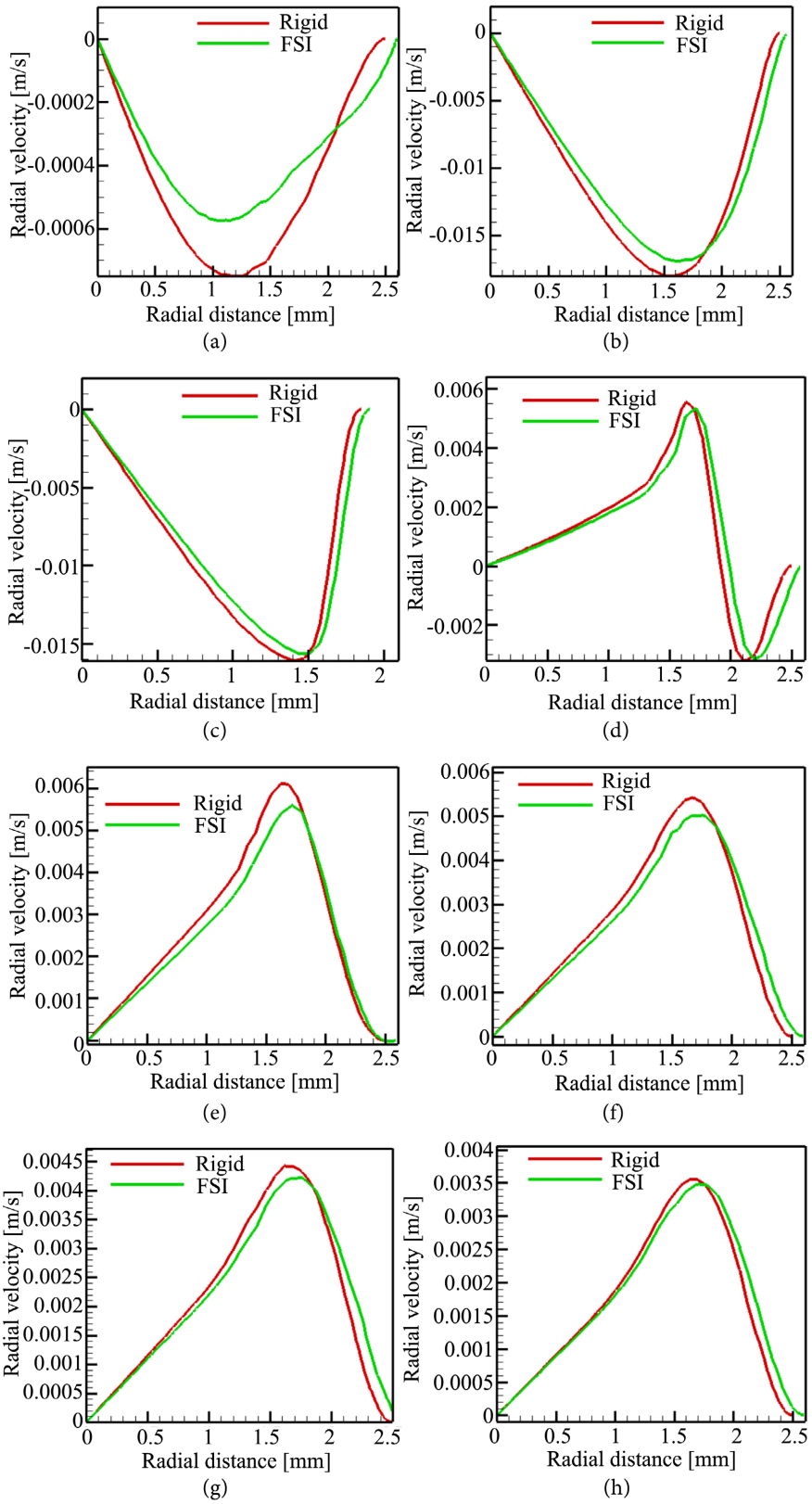

Figure 7. Radial velocity on upstream as a distance of 4 mm, 2 mm and 0 mm ((a), (b), (c)) and post stenotic zone as a distance of 2 mm, 4 mm, 6 mm, 8 mm and 10 mm ((d), (e), (f), (g), (h)) from stenosis throat of rigid and flexible walls.

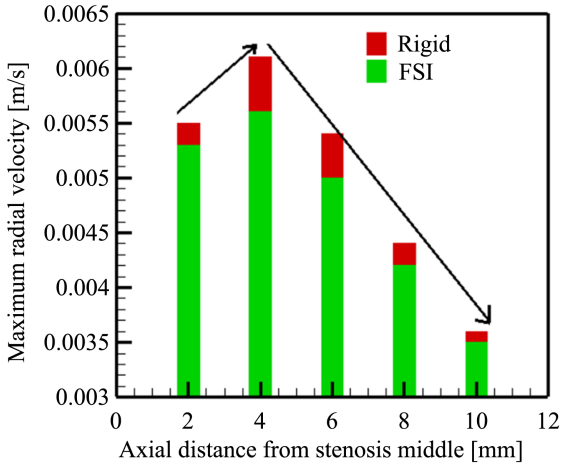

Figure 8. Maximum radial velocity at post stenotic area for rigid and elastic walls.

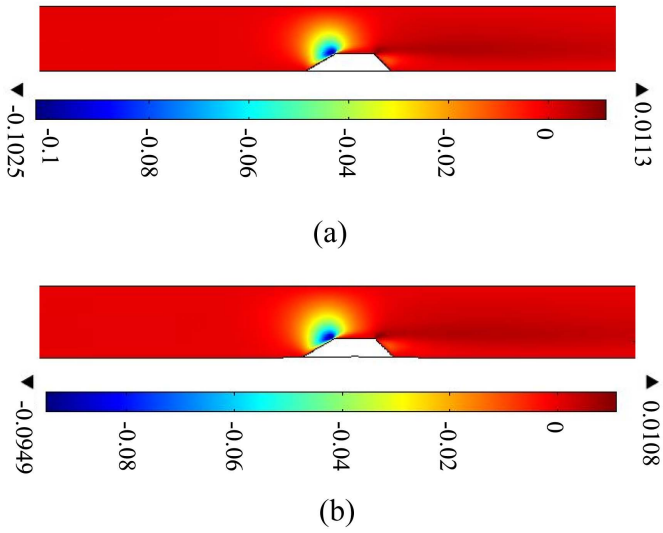

Figure 9. Radial velocity of rigid (a) and elastic walls (b) through the surface plot.

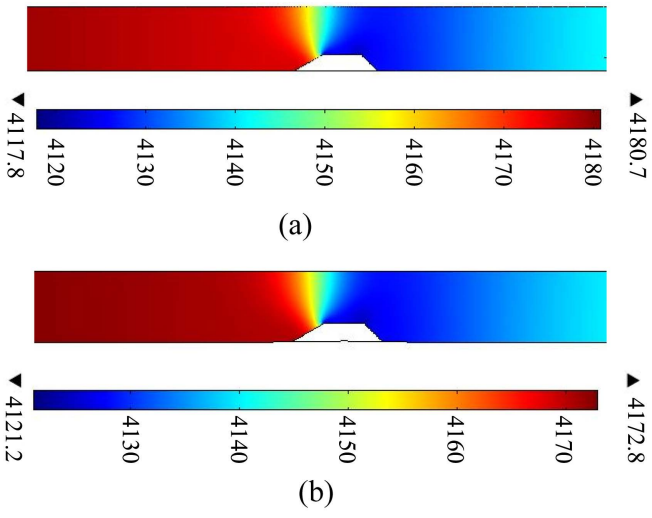

Figure 10. Surface plot of pressure for (a) rigid and (b) flexible wall.

In the current research, the effects of rigid and elastic walls on centerline velocity are investigated (Figure 12(a)). Findings show that there are similar types of flow pattern for both walls. The maximum axial velocity for rigid and flexible walls is 0.56 m/s and 0.54 m/s, respectively (Figure 12(a)). The velocity profile at the post stenosis changes greatly. This great change in velocity profile after the blockage has also been revealed in the velocity surface plot (Figure 6). The strength of velocity is high near constriction and softly declines to the downstream for all walls assumed.

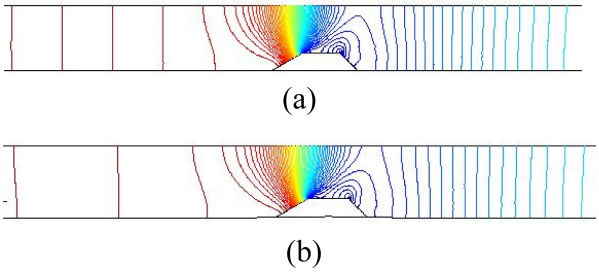

Figure 11. Pressure contour of (a) rigid and (b) flexible wall.

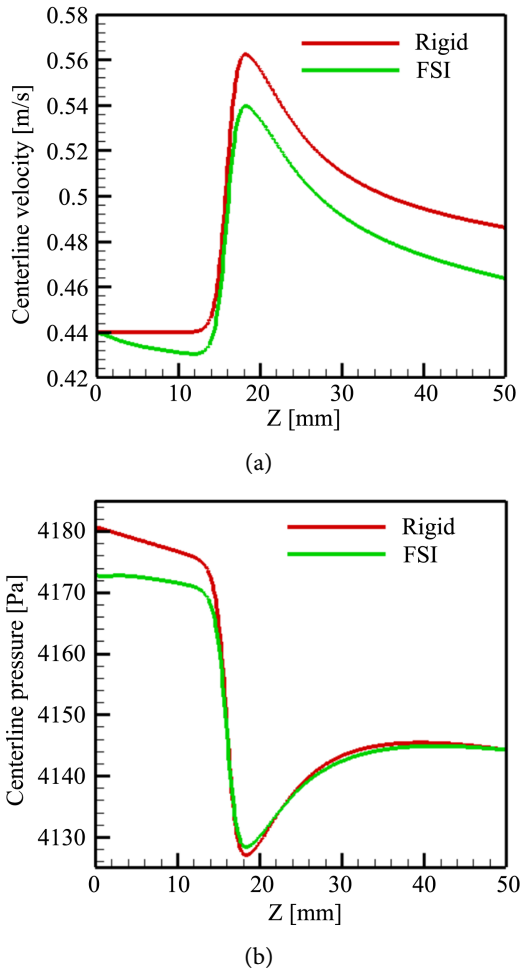

Figure 12. Velocity (a) and pressure (b) along the centerline for rigid and elastic walls.

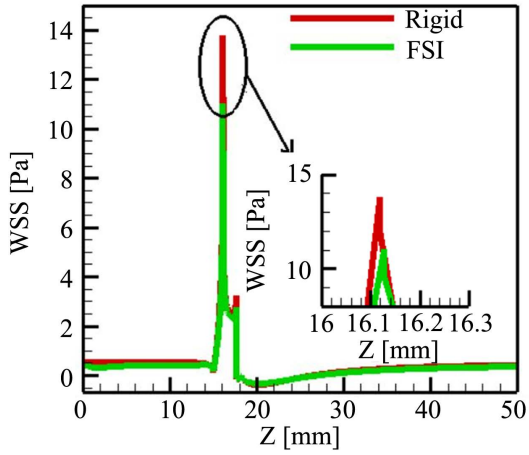

Figure 13. Shear stress along the wall through rigid and flexible walls.

The effect of the flow on the pressure at the centre of stenotic vessel has been presented in Figure 12(b). A significant pressure drop happens at the stenosis positon. Notwithstanding, pressure remains almost unaltered at the end of the artery. While there is a little rise in pressure in the post stenotic zone for all considered walls.

The impact of flow on the wall shear stress (WSS) at the stated artery is presented in Figure 13. Wall shear stress (WSS) plays an important role in the atherosclerotic analysis in arteries [13]. Nevertheless, the rupture of plaque may happen owing to maximum values of WSS. In addition, minimum and negative wall shear stress is recognized to be responsible for the plaque formation. Maximum WSS of 13.77 Pa is noticed in rigid wall while the other is 11.02 Pa in flexible wall. The larger recirculation zone is 9.8 for flexible wall while the other is 9.14 mm for rigid wall.

4. Conclusion

This research work indicates mathematical modeling of the CFD study of steady blood flow in a stenotic vessel with elastic and rigid walls whereas blood is considered to be a Newtonian fluid. The insufficient information on the variation in fluid parameters in a stenotic vessel had generated many problems to realize the heart disease trouble associated with the deposition of plaque. Comparison of the flow parameters, *i.e.*, velocity, pressure and wall shear stress are presented. Simulations are also executed to compare the variation of radial and axial velocity at upstream and downstream of the stenosis for providing a mathematical model due to the wall of rigid and elastic. The speed pattern *i.e.*, axial and radial downstream the stenosis is not the same. The maximum pressure drops for rigid and elastic wall are 54 Pa and 44 Pa respectively. It is not demanded that this research and the outcome will replace the modern approaches to the medical and surgical provision of the diseases but they can attach some additional factors as input in their detections and elementary treatment. In the future, we will study unsteady flow to detect cardiovascular diseases and its solution.

Acknowledgements

We are thankful to the editor and referees for their valuable comments.

Conflicts of Interest

The authors have no conflicts of interest.

References

[1] United Nations. Transforming Our World: The 2030 Agenda for Sustainable Development. https://www.un.org/ga/search/view_doc.asp?symbol=A/RES/70/1&Lang=E

[2] Roth, G.A., Abate, D., Abate, K.H., *et al.* (2018) Global, Regional, and National Age-Sex-Specific Mortality for 282 Causes of Death in 195 Countries and Territories, 1980-2017: A Systematic Analysis for the Global Burden of Disease Study 2017. *The Lancet*, **392**, 1736-1788. https://doi.org/10.1016/S0140-6736(18)32203-7

[3] Virani, S.S., *et al.* (2020) American Heart Association Council on Epidemiology and Prevention Statistics Committee and Stroke Statistics Subcommittee, Heart Disease and Stroke Statistics—2020 Update: A Report from the American Heart Association. *Circulation*, **141**, e139-e596. https://doi.org/10.1161/CIR.0000000000000757

[4] Tyfa, Z., Obidowski, D., Reorowicz, P., Stefanczyk, L., Fortuniak, J. and Jozwik, K. (2018) Numerical Simulations of the Pulsatile Blood Flow in the Different Types of Arterial Fenestrations: Comparable Analysis of Multiple Vascular Geometries. *Biocybernetics and Biomedical Engineering*, **38**, 228-242. https://doi.org/10.1016/j.bbe.2018.01.004

[5] Song, P.G., Fang, Z., Wang, H.Y., Cai, Y.T., Rahimi, K., Zhu, Y.J., Fowkes, F.G.R., Fowkes, F.J.I. and Rudan, I. (2020) Global and Regional Prevalence, Burden, and Risk Factors for Carotid Atherosclerosis: A Systematic Review, Meta-Analysis, and Modelling Study. *Lancet Global Health*, **8**, e721-e729. https://doi.org/10.1016/S2214-109X(20)30117-0

[6] Roy, D., Mazumder, O., Sinha, A. and Khandelwal, S. (2021) Multimodal Cardiovascular Model for Hemodynamic Analysis: Simulation Study on Mitral Valve Disorders. *PLoS ONE*, **16**, e0247921. https://doi.org/10.1371/journal.pone.0247921

[7] Ahmed, S.A. and Giddens, D.P. (1983) Velocity Measurements in Steady Flow through Axisymmetric Stenoses at Moderate Reynolds Numbers. *Journal of Biomechanics*, **16**, 505-507, 509-516. https://doi.org/10.1016/0021-9290(83)90065-9

[8] Zingaro, A., Fumagalli, I., *et al.* (2022) A Geometric Multiscale Model for the Numerical Simulation of Blood Flow in the Human Left Heart. *Discrete and Continuous Dynamical Systems*, **15**, 2391-2427. https://doi.org/10.3934/dcdss.2022052

[9] Ibrahim, M.G. (2022) Numerical Simulation to the Activation Energy Study on Blood Flow of Seminal Nanofluid with Mixed Convection Effects. *Computer Methods in Biomechanics and Biomedical Engineering*, **18**, 1-11. https://doi.org/10.1080/10255842.2022.2063018

[10] Kim, S.H., Chandran, K.B. and Chen, C.J. (1992) Numerical Simulation of Steady Flow in a Two-Dimensional Total Artificial Heart Model. *Journal of Biomechanical Engineering*, **114**, 497-503. https://doi.org/10.1115/1.2894101

[11] Kang, S., Choi, H.G. and Yoo, J.Y. (2012) Investigation of Fluid-Structure Interactions Using a Velocity-Linked P2/P1 Finite Element Method and the Generalized-α Method. International Journal for Numerical Methods in Engineering, **90**, 1529-1548.

https://doi.org/10.1002/nme.4252

[12] Kanai, H., Lizuka, M. and Sakamoto, K. (1970) One of the Problems in the Measurement of Blood Pressure by Catheter-Inserion: Wave Reflection at the Tip of the Catheter. *Medical and Biological Engineering*, **8**, 483-496. https://doi.org/10.1007/BF02477185

[13] Bajraktari, A., Bytyci, I. and Henein, M.Y. (2020) The Relationship between Coronary Artery Wall Shear Strain and Plaque Morphology: A Systematic Review and Meta-Analysis. *Diagnostics*, **10**, Article No. 91. https://doi.org/10.3390/diagnostics10020091

Nomenclature

τ : Stress tensor

u: Velocity vector

p: Pressure

ρ : Density

μ : Dynamic viscosity

CFD: Computational fluid dynamics

FSI: Fluid structure interaction

WSS: Wall shear stress